Diffusion of silver in titanium nitride: insights from density functional theory and molecular dynamics

Veniero Lenzi[a,b,*], Albano Cavaleiro[b], Filipe Fernandes[b], Luís Marques[a]

[a]*Center of Physics of Universities of Minho and Porto, University of Minho, Campus de Gualtar, Braga, 4710-057, Portugal*
[b]*University of Coimbra, CEMMPRE - Centre for Mechanical Engineering Materials and Processes, Department of Mechanical Engineering, Rua Luís Reis Santos, 3030-788, Coimbra, Portugal.*

Abstract

The use of self-lubricating titanium nitride and silver (TiN(Ag)) nanocomposite coatings is a promising way to reduce the wear of tools employed dry machining operations for hard-to-cut materials/alloys. To achieve an optimal performance, the Ag diffusion within the matrix needs to be carefully controlled, and its mechanisms clearly understood. In this paper we use density functional theory calculations to investigate Ag-related point defects, adhesion energies and Ag diffusion energy barriers in TiN bulk, surfaces and grain boundaries. Classical molecular dynamics simulations have been performed on TiN(Ag) systems using a hybrid MEAM/Mie force field, to understand the relative importance of the different diffusion processes. Our results show that the main Ag transport mechanism in TiN(Ag) nanocomposites is the surface diffusion occurring along intergranular spaces.

Keywords:

Diffusion, ab-initio, molecular dynamics, grain boundary, TiN(Ag)

---

*veniero.lenzi@fisica.uminho.pt

nanocomposite coatings, thin films.

---

1. Introduction

Titanium alloys are one of the most appealing materials in aerospace and engine industry due to their excellent mechanical properties, a high strenght-to-weight ratio combined with oxidation and corrosion resistance and low thermal expansion coefficient[1, 2]. However, their machining is difficult due to various factors that contribute to the premature tool wearing, such as the high temperatures and stresses generated on the contact, formation of building-up edges and chemical affinity between the surface and the tool [3]. This has more impact when machining is conducted without any type of liquid lubrication. A possible approach to overcome this limitation is to apply self-lubricating coatings over the surface of the cutting tools, which can also increase their lifetimes and reduce the use of liquid lubricants, with clear advantages in terms of environmental sustainability[4]. In particular, it has been recently shown that superhard titanium/silicon nitride coatings[5] with dispersed silver nanoparticles (TiSiN(Ag)) show very promising performances[6, 7, 8, 9]. In these systems, TiSiN grains are closely packed[10] and SiN is mainly found in correspondence of TiN grain boundaries(GB), while silver is found in well separated clusters. Silver acts on the contact as a lubricant, reducing both friction and adhesion between the tool and the worked surface. It is then clear that a careful control of the diffusion of Ag

within the TiSiN matrix is fundamental to obtain the best performing coating, i.e. it is desired to provide a constant lubrication during the use of the tool, and it should be avoided that silver is quickly depleted from the coating due to its outwards diffusion[11]. It is known that changing the processing parameters and the composition of the TiSiN/Ag coatings during their processing affects the diffusion rates of the lubricant[7]. Nevertheless, due to the complexity of the coating, comprising different phases and interfaces, the diffusion processes of Ag within the matrix are not yet fully understood.

In this regard, computational approaches such as ab-initio calculations and classical molecular dynamics (MD) simulations provide an effective way to model and understand the materials' behaviour. TiN has been largely investigated using ab-initio methods, with studies targeting point defects such as vacancies and substitutions[12, 13, 14, 15], adsorption properties with respect to water and oxygen[16, 17] and diffusion processes at the surface[18]. Calculations were also used to investigate the diffusion pathways along TiN GBs of copper [19] and oxygen[20]. However, to our knowledge, studies targeting Ag interactions with TiN/SiN are lacking.

MD simulations of TiN systems are generally performed using the modified embedded atom method[21, 22] (MEAM) force fields[23], as they provide a good representation of the crystal geometries and properties. Ab-initio and classical MD simulations have been used to characterize the diffusion processes of Ti and N adatoms on TiN surface[24, 25], and of N vacancies within TiN bulk[26]. As for silver, there are no MEAM parameterizations that consider TiN and Ag in the same force field, but there is a potential developed for the Ti/Ag pair[27].

The main objective of this work is to investigate the diffusion processes of Ag within the TiN matrix to understand which is the most important mechanism. The problem will be addressed using both ab-initio calculations, to have an accurate representation of the energetic aspects of diffusion, and MD simulations, to study the behaviour of Ag at high temperatures and estimate its diffusion rate.

The findings in this work will be a first step for the understanding of the much more complex TiSiN(Ag) coatings, which have been shown to have a very promising behaviour for hard to machine materials. Therefore, this paper addresses TiN(Ag) systems only, with TiN being stoichiometric, leaving the inclusion of SiN to a further work.

2. Methods

Ab-initio calculations were performed using the projector augmented wave[28] method, as implemented in VASP[29, 30] code, version 5.4.4. Density Functional Theory calculations employed the PBE functional and included the Grimme's D3 empirical dispersion correction scheme[31, 32], which provides a good representation of non covalent interactions, such as those of Ag at the TiN surface. Defect energies in bulk TiN were calculated using a 64-atom TiN supercell. Lattice constants and atom positions were fully relaxed until all atomic forces converged to 10 meV/atom. A 6x6x6 K-point grid was used with the Monhorst-Pack sampling scheme, and a cutoff of 800 eV. Surface defects were calculated considering a 8-layer thick slab, the inner three of which were frozen, and a vacuum layer of 15 Å. The slab plane normal is parallel to the z axis, so that a 6x6x1 k-point grid was used. Defect energies

E_d were calculated using the formula

$$E_d = E(X + d) - \sum_i N_i \mu_i,$$ (1)

where $E(X + d)$ is the energy of the system with the defect and N_i is the number of atoms of species i with chemical potential μ_i.

Chemical potentials were obtained with the formula

$$\mu_{TiN} = \mu_{Ti} + \mu_N,$$ (2)

where for Ti-rich and N-rich environments, the formation energies of bulk hcp Ti and N dimer were used as reference chemical potentials for Ti and N, respectively. For Ag, the reference energy was assumed to be that of fcc Ag.

For surfaces and GBs, the defect energy was calculated instead using the formula

$$E_d = E(X + d) - E(X) + \sum_i \delta N_i \mu_i,$$ (3)

where $E(X)$ represents the energy of the defect-free system and δN_i is the difference in the number of atoms of i-th species, μ_i being the corresponding chemical potential. In this way, the surface/interface energy contributions are cancelled out. Supercells containing 320 atoms were used for grain boundary calculations, with the grain boundary at the middle and free surfaces separated by 20 atomic layers on each side. In this case, a grid of 5x5x1 k-points was used and the cutoff was reduced to 600 eV. In addition, the convergence criterion for force relaxation was increased to 20 meV/atom.

Molecular dynamics simulations were performed using LAMMPS[33]. A hybrid MEAM[21, 22] forcefield, with the addition of a Mie[34] term to describe N-Ag interactions, was used. The files containing all the parameters

to run TiN/Ag simulations are provided in supplementary material. All simulations used periodic boundary conditions and were conducted under NPT conditions, implemented by a Nosé-Hoover[35, 36] thermostat and barostat, with damping constants of 0.1 and 1 ps, respectively. A timestep of 1 fs was used. In the case of surface calculations, in which the z axis always identifies the surface normal, the barostat acted only on the x and y direction. TiN systems of 1000 atoms were used to calculate both the point defect energy in bulk and the surface adhesion properties. For the GB simulations, we used 1600-atom TiN boxes. The defect and adhesion energies were calculated at 0 K, after an energy minimization. For Ag diffusion calculations, 12 statistically independent runs of 1 ns were employed for each system and temperature. Samples were equilibrated at the target temperature for 100 ps, and then the data production run was carried on for 1 ns. In all cases, only a single Ag atom was added to the TiN systems. Diffusion jump rates were calculated by inspecting the mean square displacement of the Ag atoms, and manually counting the jumps.

3. Results and discussion

3.1. Ab-initio calculations

3.1.1. Defect formation energy in bulk TiN

In this section, the most likely diffusion mechanism to be present is TiN(Ag) nanocomposites, based upon density functional theory calculations, is presented.

It is expected that bulk diffusion, i.e. diffusion of Ag atoms within the TiN matrix, is a highly unfavourable process. To confirm this, the energies

of either the silver substitution in TiN lattice sites or the silver interstitials were calculated in bulk TiN. As shown in figure 1, the interstitial defects are strongly unfavoured, with a formation energy of 11.6 eV. Positive energies were also found for silver substitutions.
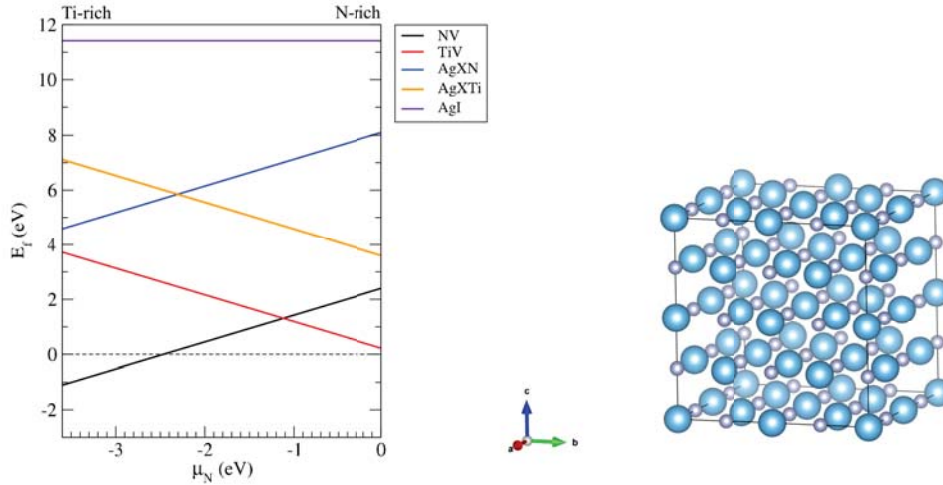

Figure 1: On the left, formation energies of Ti (TiV) and N (NV) vacancies, Ag substitutions of Ti (AgXTi) and N (AgXN) and Ag interstitial (AgI) defects in bulk TiN, expressed as a function of the chemical potential of nitrogen, given with respect to half of the N_2 energy. On the right, a representation of the supercell employed for calculations, with Ti atoms being the larger spheres (in blue) and N atoms the smaller ones (in grey).

These results indicate that silver does not diffuse through the TiN matrix and that a defect-mediated diffusion is also unlikely, at least at low temperatures and normal pressure conditions. In fact, experimental evidence seem to confirm this, with Ag mainly found along GBs and within intercolumnar voids after annealing a sputtered deposited TiN(Ag) coating[7].

7

It is important to calculate the defect formation energies in correspond-ence to a (001) surface. Comparing with the energies obtained in bulk, similar values are found for N and Ti vacancies. Conversely,the formation of silver substitutions is favoured at the surface, with a formation energy of 0.27 eV for the N substitution and 0.76 eV for the Ti one. Interestingly, as it is shown in figure 2, Ag surface substitutions are not occupying exactly the lattice sites, but resting slightly above the surface defects.
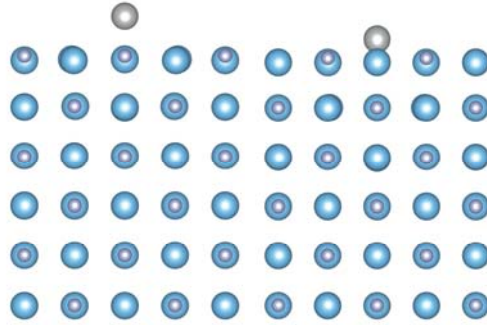

Figure 2: Final configuration of Ag substitution defects at the TiN surface, for a N-substitution (left) and a Ti-substitution (right).

To investigate the surface diffusion properties of Ag, the potential energy landscape of an Ag atom diffusing over a (001) TiN surface was calculated. An 8x8 grid spanning the TiN unit surface cell was constructed, and the silver atom was placed on top of each grid point. Further, the system was relaxed while keeping the cell parameters and the Ag atom X and Y coordinates fixed. As shown in figure 3, the Ag PES is relatively shallow. The minimum, taken as reference energy, is located at the centre of the cell, where the Ag adsorption energy is 1.51 eV. Other minima are located over Ti atom, with
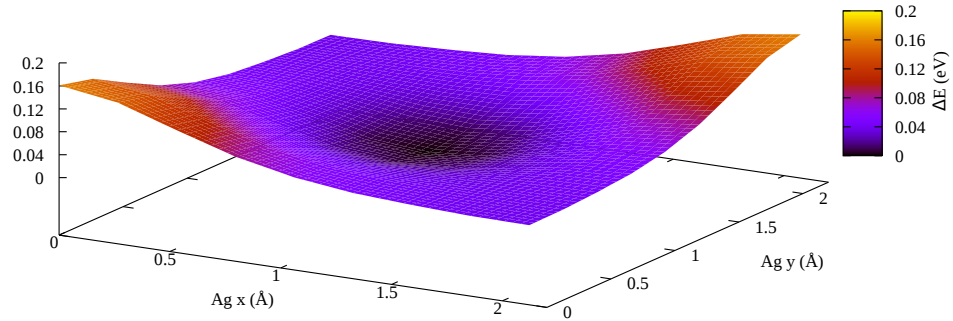
Figure 3: Potential energy landscape of a Ag atom on the TiN (001) surface. The 0 of the energy corresponds to the Ag adsorption energy at the minimum position, located in the middle of the surface cell, and corresponding to 1.51 eV. The origin corresponds to a nitrogen atom.

an energy only 0.038 eV larger. On the other hand, there is one maximum corresponding to the N-top position for Ag, which has an energy 0.161 eV larger than the minimum. Hence Ag atoms can easily diffuse on TiN along diffusion pathways connecting Ti atoms. Low energy values for surface silver substitutions indicate that surface vacancies might stop the diffusion of Ag atoms, providing potential nucleation sites for Ag grain reconstruction.

3.1.3. Ag in grain boundaries

Another possible diffusion pathway within TiN matrix is along tilt GBs. Due to the production technique of the TiN matrix, TiN grains are organized in columns. Such columns are generally separated by few nm of empty space, the intercolumnar space, and could also be in tight contact by means of GBs. In the first case of large separation the diffusion along the crystal edge is

9

essentially a surface one, already investigated in the previous section, while in the second case, the diffusion mechanism is clearly different, as it occurs along 1-d channels.

Although many different GBs structures are possible, depending upon the angle made by the crystal planes of the grains in contact, we restricted here our study to the two most stable tilt GBs[19], i.e. those of Duffy-Tasker and Kingery types, shown in figure 4. Indeed, these GBs are characterized by the presence of 1-d channels, parallel to the GB-plane, that could host the diffusing species.

The energy to insert an Ag atom in the center of a GB channel was calculated. As expected, the insertion energy is lower in the case of the Duffy-Tasker type GB, with a value of 1.50 eV, which compares with 3.89 eV for the Kingery type GB.

These results indicate that Ag atoms can enter more easily inside a Duffy-Tasker GB channel, due to the larger space they provide. To gain further insight, the diffusion energy barriers along the GBs were calculated using the Nudged Elastic Band (NEB) method[37], employing 5(Kingery) and 6(Duffy-Tasker) images. As can be appreciated in figure 5, there is a large energy barrier along the Kingery GBs channel of 3 eV, whereas one of 0.24 eV is found in the other case. Hence, based upon energetic considerations, Ag can diffuse along Duffy-Tasker type GBs much more easily than along Kingery ones.
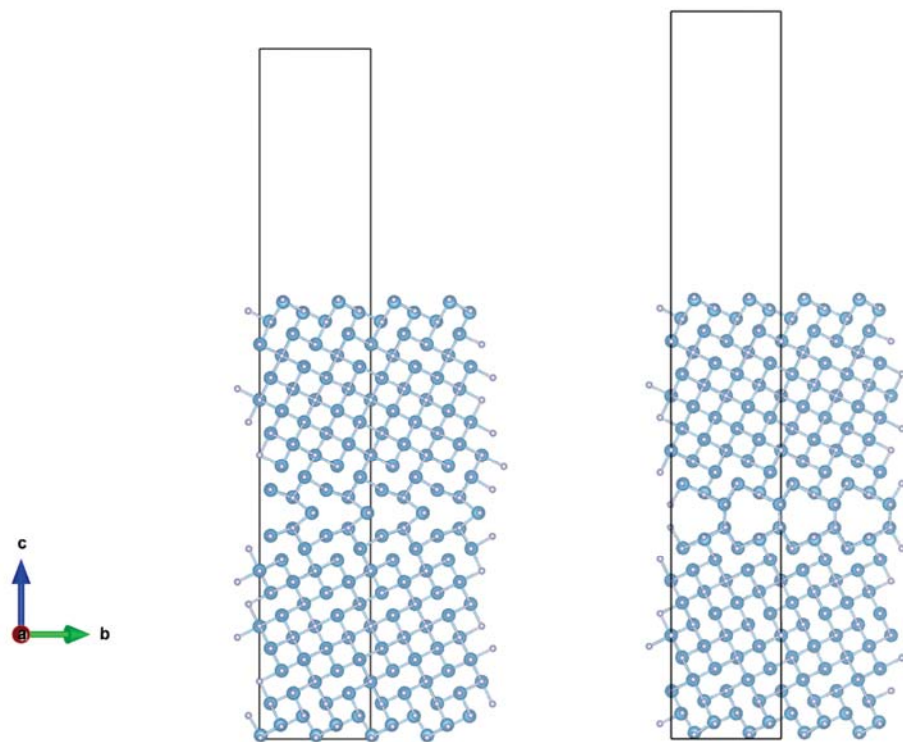
Figure 4: The Kingery type grain boundary is represented on the left, while the Duffy-Tasker type on the right. In both cases, the GBs are perpendicular to the c axis and Ag atom diffusion can occur only along the a axis, perpendicular to the sheet plane.
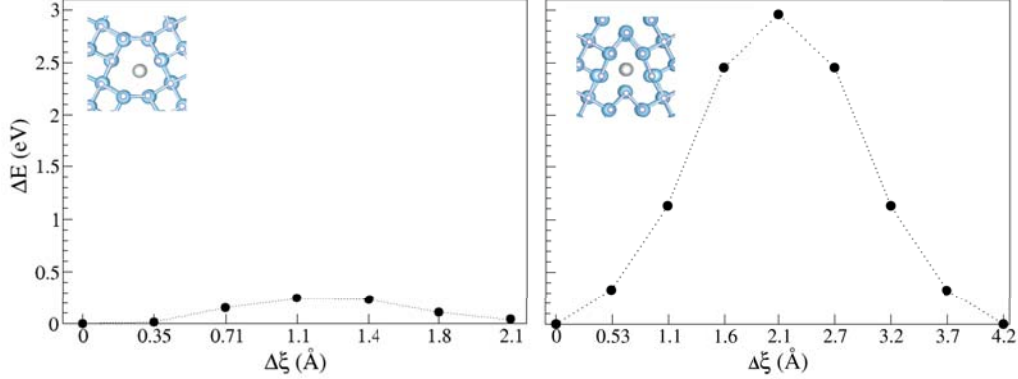
Figure 5: Energy barriers for diffusion along GB in the case of Duffy-Tasker (left) and Kingery (right) type GB, represented in insets. In the abscissa, $\Delta\xi$ represents the Ag displacement along the GB channel, i.e normal to the sheet plane.

3.2. Molecular dynamics simulations

3.2.1. Force Field derivation

To simulate the TiN/Ag nanocomposites the interaction parameters between N and Ag are needed. However, the lack of stable N/Ag structures complicates the parametrization of a MEAM potential for this pair. Beside this, MEAM forcefields are generally working best when applied to study bulk materials, whereas surface properties such as adhesion of single atoms and defect formation energies are less accurate. Bearing this in mind, we adopted the forcefield from the group of Sangiovanni[26] and collaborators for TiN, and combined it with the one from Zhou[27] to get the Ti-Ag pair potential. For the N-Ag interaction, a Mie potential was considered:

$$U(r) = E_0 \cdot \left[\left(\frac{\sigma}{r} \right)^{0.7} - \left(\frac{\sigma}{r} \right)^{0.35} \right], \tag{4}$$

12

where σ is equal to 3.08 Å, and $E_0 = 4.8$ eV. A cutoff $r_c \equiv \sigma$ was considered to ignore the attractive part of the potential. Those parameters were derived firstly by optimizing the MD silver substitution formation energies in bulk TiN. Next, the Mie parameters were modified in order to best reproduce the PES of figure 3. The Ti-Ag α[21] parameter was also reduced from 5.85 to 5.05. Finally, the N-Ag screening parameters were assumed to be as those of N-Ti[38].

In table 1 are reported the energies of the Ag defects calculated using the proposed force field. The agreement with DFT data is remarkable in all cases, with the bulk Ag interstitial energy reproduced almost exactly, while a slight overestimation of the surface substitution energies and underestimation of adhesion energies is found. In the other cases, the agreement with DFT is less accurate, but still good. The largest deviations are observed for Ag substitutions in bulk, which are underestimated, and for the Duffy-Tasker GB Ag interstitial. A different choice for the Mie parameters could amend this, but at the cost of worsening the surface energies.

The PES of an Ag atom on a TiN surface was calculated using the hybrid forcefield developed and was compared with the one of figure 3, obtained using DFT. Their difference is reported in figure 6. We can see that the MD results reproduces most of the features observed, namely the minima over the centre and Ti atoms and the maxima over N atoms. However, the maximum is overestimated by 0.16 eV . Additionally, metastable positions appeared at the midpoints of the Ti-N directrices, and small energy barriers of 0.1 eV appeared in proximity of Ti atoms.

Finally, the diffusion energy barriers along the GBs considered here were

Defect	DFT Energy (eV)	MD Energy (eV)
Bulk: Ag interstitial	11.61	10.98
Bulk: AgXN	5.57	3.12
Bulk: AgXTi	3.26	2.11
Duffy-Tasker GB: Ag interstitial	1.50	0.59
Kingery GB: Ag interstitial	3.89	3.78
Surface: AgXN	0.27	0.40
Surface: AgXTi	0.76	1.04
Surface: Ag adsorption(Hollow)	1.51	1.11

Table 1: Comparison of Ag substitution, interstitials and adsorption energies calculated using DFT and MD.
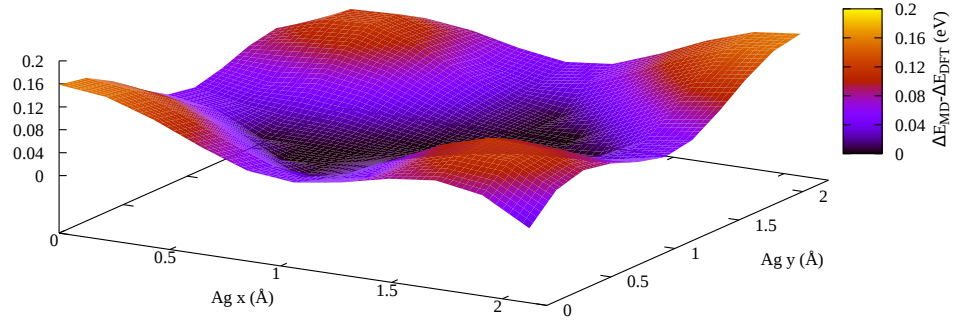

Figure 6: Difference between the potential energy landscape of a Ag atom on the TiN (001) surface calculated using MD and the one of figure 3, obtained using DFT. The origin corresponds to a nitrogen atom.

also estimated using MD and compared with the NEB results, finding a value of 0.55 eV for the Duffy-Tasker barrier and of 3.59 for the Kingery one. Both barriers are larger than the DFT ones, but their ordering is still preserved.

Summarizing, the introduced hybrid forcefield reproduces the most important features of Ag diffusion as observed using DFT. Although there is an overestimation of diffusion barriers, we can see that it is consistent in both DT GBs and surface barriers. The underestimation of Ag substitutions energies in bulk TiN is not relevant as long as the temperature and pressure ranges investigated do not allow for defect formation, as in our case.

3.2.2. Diffusion rates along grain boundaries and surfaces

In figure 7, we report the jump rates as a function of temperature for a single atom diffusion along a TiN surface and along the Duffy-Tasker GB channel. For low temperatures, the diffusion dynamic is discontinuous, with the Ag atom resting in one low-energy site and then suddenly moving to another one. As long as the dynamic is discrete, the jump rates could provide a good estimate of the diffusion kinetics. It should be kept in mind that each jump does not necessarily correspond to a displacement from a favourable site to its next-neighbour one, but longer displacements are possible and were indeed observed. At higher temperatures, especially for the surface diffusion, it was not possible to count the jumps because the Ag atom dynamics assumed a continuous-like aspect, making it difficult to quantify. These results show that the surface diffusion is clearly the fastest, especially at low temperatures. Regarding the diffusion along GBs, we could observe diffusion only for the large (Duffy-Tasker) GB, as could be expected by the larger Ag insertion energy for the KG one.
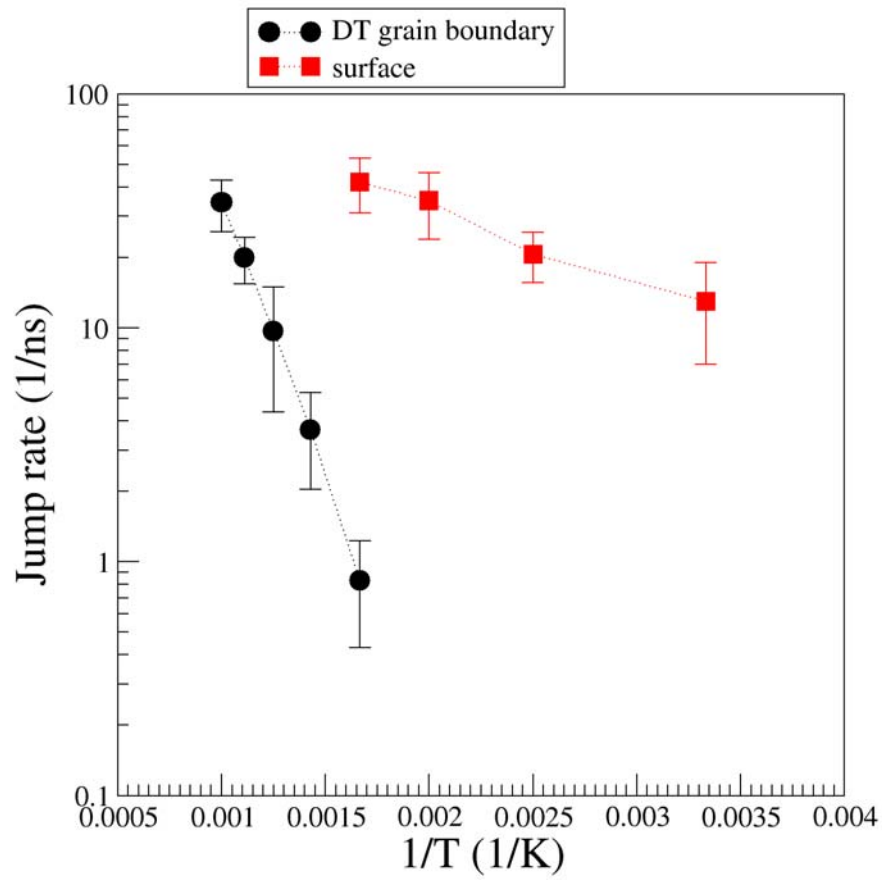
Figure 7: Jump rates (in jumps/ns) calculated from MD simulation for DT GB and TiN surface. The error bars represent one standard deviation from the computed value.

4. Conclusions

The adhesion and diffusion energies of Ag within TiN/Ag nanocomposites were studied by means of ab-initio calculations and classical MD simulations, finally allowing to assess the different Ag diffusion mechanisms in a pure TiN matrix.

Bulk and defect-mediated diffusion is the least probable mechanism, due to the high formation energies involved in the formation of defects, especially silver substitutions. Our calculations also indicate that Ag cannot assume interstitial positions, as those are energetically very unfavorable. It is thus safe to assume that Ag does not penetrate the TiN matrix, but could only diffuse on surfaces and GBs.

Concerning surface diffusion, our PES calculation demonstrates that Ag atoms can freely diffuse on surfaces along Ti-Ti directrices and might be stopped by the presence of surface point defects, such as vacancies. GB diffusion appears to be an important mechanism only when GBs have enough inter-granular space to host an Ag atom, such as in the DT type, while diffusion along Kingery GB seems unfavourable.

A hybrid MEAM/Mie forcefield for MD simulations was developed considering Ti,N and Ag within the same framework, with an emphasis on surface properties during the parametrization. Notwithstanding the simple treatment of N-Ag interactions, MD results were in good agreement with ab-initio calculations. Thus, by measuring the jump rates of GB versus surface diffusion, it was found that surface diffusion is clearly the fastest process, meaning that any strategy aimed at reducing the Ag leakage from the coating should hinder this mechanism.

17

Acknowledgements

References

[1] R. M'Saoubi, D. Axinte, S. L. Soo, C. Nobel, H. Attia, G. Kappmeyer, S. Engin, W.-M. Sim, High performance cutting of advanced aerospace alloys and composite materials, CIRP Annals 64 (2) (2015) 557 – 580. doi:https://doi.org/10.1016/j.cirp.2015.05.002.
URL http://www.sciencedirect.com/science/article/pii/S0007850615001419

[2] N. Khanna, J. Davim, Design-of-experiments application in machining titanium alloys for aerospace structural components, Measurement 61 (2015) 280 – 290. doi:https://doi.org/10.1016/j.measurement.2014.10.059.
URL http://www.sciencedirect.com/science/article/pii/S0263224114005284

[3] A. Pramanik, Problems and solutions in machining of titanium alloys, The International Journal of Advanced Manufacturing Technology 70 (5) (2014) 919–928. doi:10.1007/s00170-013-5326-x.
URL https://doi.org/10.1007/s00170-013-5326-x

[4] S. Debnath, M. M. Reddy, Q. S. Yi, Environmental friendly cutting fluids and cooling techniques in machining: a review, Journal of Cleaner Production 83 (2014) 33 – 47. doi:https://doi.org/10.1016/j.jclepro.2014.07.071.
URL http://www.sciencedirect.com/science/article/pii/S0959652614007999

[5] S. Veprek, M. J. Veprek-Heijman, Industrial applications of superhard nanocomposite coatings, Surface and Coatings Technology 202 (21) (2008) 5063 – 5073. doi:https://doi.org/10.1016/j.surfcoat.2008.05.038.
URL http://www.sciencedirect.com/science/article/pii/S0257897208004064

[6] S. Calderon Velasco, A. Cavaleiro, S. Carvalho, Functional properties of ceramic-ag nanocomposite coatings produced by magnetron sputtering, Progress in Materials Science 84 (2016) 158 – 191. doi:https://doi.org/10.1016/j.pmatsci.2016.09.005.
URL http://www.sciencedirect.com/science/article/pii/S0079642516300627

[7] D. Cavaleiro, S. Carvalho, A. Cavaleiro, F. Fernandes, Tisin(ag) films deposited by hipims working in doms mode: Effect of ag content on structure, mechanical properties and thermal stability, Applied Surface Science 478 (2019) 426 – 434. doi:https://doi.org/10.1016/j.apsusc.2019.01.174.
URL http://www.sciencedirect.com/science/article/pii/S0169433219301680

[8] D. Cavaleiro, D. Veeregowda, A. Cavaleiro, S. Carvalho, F. Fernandes, High temperature tribological behaviour of tisin(ag) films deposited by hipims in doms mode, Surface and Coatings Technology 399 (2020) 126176. doi:https://doi.org/10.1016/j.surfcoat.2020.126176. URL http://www.sciencedirect.com/science/article/pii/S0257897220308458

[9] D. Cavaleiro, D. Figueiredo, C. Moura, A. Cavaleiro, S. Carvalho, F. Fernandes, Machining performance of tisin(ag) coated tools during dry turning of tial6v4 aerospace alloy, Ceramics International (2021). doi:https://doi.org/10.1016/j.ceramint.2021.01.021. URL http://www.sciencedirect.com/science/article/pii/S0272884221000304

[10] F. Fernandes, S. Calderon V., P. Ferreira, A. Cavaleiro, J. Oliveira, Low peak power deposition regime in hipims: Deposition of hard and dense nanocomposite ti-si-n films by doms without the need of energetic bombardment, Surface and Coatings Technology 397 (2020) 125996. doi:https://doi.org/10.1016/j.surfcoat.2020.125996. URL http://www.sciencedirect.com/science/article/pii/S0257897220306654

[11] C. Muratore, A. Voevodin, J. Hu, J. Zabinski, Tribology of adaptive nanocomposite yttria-stabilized zirconia coatings containing silver and molybdenum from 25 to 700°c, Wear 261 (7) (2006) 797 – 805. doi:https://doi.org/10.1016/j.wear.2006.01.029. URL http://www.sciencedirect.com/science/article/pii/S0043164806000317

[12] L. Tsetseris, N. Kalfagiannis, S. Logothetidis, S. T. Pantelides, Structure and interaction of point defects in transition-metal nitrides, Phys. Rev.

B 76 (2007) 224107. doi:10.1103/PhysRevB.76.224107.
URL `https://link.aps.org/doi/10.1103/PhysRevB.76.224107`

[13] V. Razumovskiy, M. Popov, H. Ding, J. Odqvist, Formation and interaction of point defects in group ivb transition metal carbides and nitrides, Computational Materials Science 104 (2015) 147 – 154. doi:https://doi.org/10.1016/j.commatsci.2015.03.042.
URL `http://www.sciencedirect.com/science/article/pii/S0927025615002153`

[14] R. Bès, Y. Pipon, N. Millard-Pinard, S. Gavarini, M. Freyss, First-principles study of rare gas incorporation in titanium nitride, Phys. Rev. B 87 (2013) 024104. doi:10.1103/PhysRevB.87.024104.
URL `https://link.aps.org/doi/10.1103/PhysRevB.87.024104`

[15] S. Carara, L. Thesing, P. Piquini, First principles study of vacancies and al substitutional impurities in -tin, Thin Solid Films 515 (4) (2006) 2730 – 2733. doi:https://doi.org/10.1016/j.tsf.2006.03.028.
URL `http://www.sciencedirect.com/science/article/pii/S0040609006004640`

[16] S. Sanyal, U. V. Waghmare, J. A. Ruud, Adsorption of water on tin (100), (110) and (111) surfaces: A first-principles study, Applied Surface Science 257 (15) (2011) 6462 – 6467. doi:https://doi.org/10.1016/j.apsusc.2011.02.042.
URL `http://www.sciencedirect.com/science/article/pii/S0169433211002339`

[17] F. Guo, J. Wang, Y. Du, J. Wang, S.-L. Shang, S. Li, L. Chen, First-principles study of adsorption and diffusion of oxygen on surfaces of tin, zrn and hfn, Applied Surface Science 452 (2018) 457 – 462.

doi:https://doi.org/10.1016/j.apsusc.2018.05.052.

URL http://www.sciencedirect.com/science/article/pii/S016943321831328X

[18] Y. Ren, X. Liu, X. Tan, E. Westkämper, Adsorption and pathways of single atomistic processes on tin (111) surfaces: A first principle study, Computational Materials Science 77 (2013) 102 – 107. doi:https://doi.org/10.1016/j.commatsci.2013.04.036.

URL http://www.sciencedirect.com/science/article/pii/S0927025613002085

[19] M. N. Popov, A. S. Bochkarev, V. I. Razumovskiy, P. Puschnig, J. Spitaler, Point defects at the $\Sigma5(012)[100]$ grain boundary in tin and the early stages of cu diffusion: An ab initio study, Acta Materialia 144 (2018) 496 – 504. doi:https://doi.org/10.1016/j.actamat.2017.11.005.

URL http://www.sciencedirect.com/science/article/pii/S1359645417309485

[20] K. P. McKenna, Structure, electronic properties, and oxygen incorporation/diffusion characteristics of the Σ£ 5 tin(310)[001] tilt grain boundary, Journal of Applied Physics 123 (7) (2018) 075301. arXiv:https://doi.org/10.1063/1.5016626, doi:10.1063/1.5016626.

URL https://doi.org/10.1063/1.5016626

[21] M. I. Baskes, Modified embedded-atom potentials for cubic materials and impurities, Phys. Rev. B 46 (1992) 2727–2742. doi:10.1103/PhysRevB.46.2727.

URL https://link.aps.org/doi/10.1103/PhysRevB.46.2727

[22] B.-J. Lee, M. Baskes, H. Kim, Y. Koo Cho, Second nearest-neighbor modified embedded atom method potentials for bcc transition metals,

Phys. Rev. B 64 (2001) 184102. doi:10.1103/PhysRevB.64.184102.

URL `https://link.aps.org/doi/10.1103/PhysRevB.64.184102`

[23] Y.-M. Kim, B.-J. Lee, Modified embedded-atom method interatomic potentials for the ti–c and ti–n binary systems, Acta Materialia 56 (14) (2008) 3481 – 3489. doi:https://doi.org/10.1016/j.actamat.2008.03.027.

URL `http://www.sciencedirect.com/science/article/pii/S135964540800236X`

[24] D. G. Sangiovanni, D. Edström, L. Hultman, V. Chirita, I. Petrov, J. E. Greene, Dynamics of ti, n, and tin$_x$ ($x = 1 - -3$) admolecule transport on tin(001) surfaces, Phys. Rev. B 86 (2012) 155443. doi:10.1103/PhysRevB.86.155443.

URL `https://link.aps.org/doi/10.1103/PhysRevB.86.155443`

[25] D. Sangiovanni, D. Edström, L. Hultman, I. Petrov, J. Greene, V. Chirita, Ti adatom diffusion on tin(001): Ab initio and classical molecular dynamics simulations, Surface Science 627 (2014) 34 – 41. doi:https://doi.org/10.1016/j.susc.2014.04.007.

URL `http://www.sciencedirect.com/science/article/pii/S0039602814001010`

[26] D. G. Sangiovanni, B. Alling, P. Steneteg, L. Hultman, I. A. Abrikosov, Nitrogen vacancy, self-interstitial diffusion, and frenkel-pair formation/dissociation in b1 tin studied by ab initio and classical molecular dynamics with optimized potentials, Phys. Rev. B 91 (2015) 054301. doi:10.1103/PhysRevB.91.054301.

URL `https://link.aps.org/doi/10.1103/PhysRevB.91.054301`

[27] Y. Zhou, R. Smith, S. D. Kenny, A. L. Lloyd, Development of an em-

pirical interatomic potential for the ag–ti system, Nuclear Instruments and Methods in Physics Research Section B: Beam Interactions with Materials and Atoms 393 (2017) 122 – 125, computer Simulation of Radiation effects in Solids Proceedings of the 13 COSIRES Loughborough, UK, June 19-24 2016. doi:https://doi.org/10.1016/j.nimb.2016.10.030.
URL `http://www.sciencedirect.com/science/article/pii/S0168583X16304529`

[28] P. E. Blöchl, Projector augmented-wave method, Phys. Rev. B 50 (1994) 17953–17979. doi:10.1103/PhysRevB.50.17953.
URL `https://link.aps.org/doi/10.1103/PhysRevB.50.17953`

[29] G. Kresse, J. Furthmüller, Efficient iterative schemes for ab initio total-energy calculations using a plane-wave basis set, Phys. Rev. B 54 (1996) 11169–11186. doi:10.1103/PhysRevB.54.11169.
URL `https://link.aps.org/doi/10.1103/PhysRevB.54.11169`

[30] G. Kresse, D. Joubert, From ultrasoft pseudopotentials to the projector augmented-wave method, Phys. Rev. B 59 (1999) 1758–1775. doi:10.1103/PhysRevB.59.1758.
URL `https://link.aps.org/doi/10.1103/PhysRevB.59.1758`

[31] S. Grimme, J. Antony, S. Ehrlich, H. Krieg, A consistent and accurate ab initio parametrization of density functional dispersion correction (dft-d) for the 94 elements h-pu, The Journal of Chemical Physics 132 (15) (2010) 1–19. doi:10.1063/1.3382344.
URL `http://scitation.aip.org/content/aip/journal/jcp/132/15/10.1063/1.3382344`

[32] S. Grimme, S. Ehrlich, L. Goerigk, Effect of the damping function in

dispersion corrected density functional theory, Journal of Computational Chemistry 32 (7) (2011) 1456–1465. doi:10.1002/jcc.21759.

URL http://dx.doi.org/10.1002/jcc.21759

[33] S. Plimpton, Fast parallel algorithms for short-range molecular dynamics, Journal of Computational Physics 117 (1) (1995) 1 – 19. doi:10.1006/jcph.1995.1039.

URL http://www.sciencedirect.com/science/article/pii/S002199918571039X

[34] G. Mie, Zur kinetischen theorie der einatomigen körper, Annalen der Physik 316 (8) (1903) 657–697. arXiv:https://onlinelibrary.wiley.com/doi/pdf/10.1002/andp.19033160802, doi:https://doi.org/10.1002/andp.19033160802.

URL https://onlinelibrary.wiley.com/doi/abs/10.1002/andp.19033160802

[35] W. G. Hoover, Canonical dynamics: Equilibrium phase-space distributions, Physycal Review A 31 (1985) 1695–1697. doi:10.1103/PhysRevA.31.1695.

URL http://link.aps.org/doi/10.1103/PhysRevA.31.1695

[36] M. Parrinello, A. Rahman, Polymorphic transitions in single crystals: A new molecular dynamics method, Journal of Applied Physics 52 (12) (1981) 7182–7190. doi:10.1063/1.328693.

URL http://scitation.aip.org/content/aip/journal/jap/52/12/10.1063/1.328693

[37] D. Sheppard, R. Terrell, G. Henkelman, Optimization methods for finding minimum energy paths, The Journal of Chemical Physics 128 (13) (2008) 134106. arXiv:https://doi.org/10.1063/1.2841941,

doi:10.1063/1.2841941.

URL https://doi.org/10.1063/1.2841941

[38] B.-J. Lee, W.-S. Ko, H.-K. Kim, E.-H. Kim, The modified embedded-atom method interatomic potentials and recent progress in atomistic simulations, Calphad 34 (4) (2010) 510 – 522. doi:https://doi.org/10.1016/j.calphad.2010.10.007.

URL http://www.sciencedirect.com/science/article/pii/S0364591610000817